

Nondestructive High-Power-High-Temperature Raman Spectroscopy for Probing Microscopic Structural Variations in CZTSe Alloys

Qiong Chen¹, Sergio Bernardi², and Yong Zhang¹

¹Department of Electrical and Computer Engineering, and Energy Production and Infrastructure Center (EPIC), The University of North Carolina at Charlotte, Charlotte, NC 28223, USA

²Semiconductor Materials Specialist, C.so Trapani 10, 10139 Turin, Italy.

ABSTRACT

Even though absorber layers fabricated by different methods may yield comparable efficiencies and appear to be similar under conventional probes, such as low power Raman, PL, XRD, they could in fact be quite different in their microscopic structures. We have developed a novel nondestructive spectroscopy approach, high-power-high-temperature (HPHT) Raman spectroscopy, which is capable of revealing the microscopic structural variations of complex alloys like CZTSe over a large area. CZTSe films prepared by sputtering and co-evaporation methods were examined and compared in both lateral and depth directions. In general, high power (HP) illumination brought qualitatively different changes to the CZTSe samples, not only in the CZTSe Raman peaks but also in the secondary phases, which suggests that there is some subtle microscopic differences between the two types of samples. In addition, 2D Raman mapping revealed a larger spatial extension of the local heating effect caused by HP illumination in the sputtered film, which also indicates that two nominally similar films might have different thermal conductivities. High temperature (HT) measurement, which offers uniform heating as opposed to local heating with high power, further enhances the capability of the approach.

INTRODUCTION

Raman spectroscopy is an effective tool for chemical composition and structural analyses. It is used under the assumption that the probe light intensity is sufficiently weak so that the perturbation will not lead any structural change. In HP Raman spectroscopy, a tightly focused CW laser with a power density that is just high enough to introduce a local structural change is used. Raman spectra collected with lower power (LP) is compared before and after to measure the change introduced by HP illumination. HP Raman spectroscopy can reveal some subtle but important structural differences in two samples that might otherwise appear to be indistinguishable under the normal probes. For instance, some structural or chemical fluctuations are too feeble to be detectable or distinguishable in the as-grown sample or between different ones, but are signified after being modified by the HP illumination. Complementary information can be obtained by further applying HT Raman spectroscopy. The combination of the HP and HT Raman spectroscopy, in conjunction with the high spatial resolution of the confocal optics, is a very powerful approach for probing the structural variation and inhomogeneity, in particular in a complex alloy like CZTSe, with high sensitivity and efficiency, and complementary to TEM and other laser spectroscopy techniques.

EXPERIMENT

All μ -Raman measurements were performed with Horiba Jobin Yvon HR800 confocal Raman system with a CCD detector using 532 nm laser. The room temperature Raman measurement was performed in air, with a 100x objective lens whose numerical aperture is 0.9. The diffraction limit laser spot size is 0.76 μm , and the spatial resolution of the measurement is about half of the spot size. For HT measurements, a 50x long working distance lens with 0.5 numerical aperture was used, and the samples were evenly heated in nitrogen atmosphere by Linkam TS1500 heating system with temperature control accuracy of 1 $^{\circ}\text{C}$.

Three different samples were compared: bare CZTSe film CZTSe_97 (S1), bare CZTSe film M3599_12 (S2) and CZTSe solar cell device M3602_21 (S3). Sample S1 was prepared by selenizing the metal stacks which composed of 300 nm Mo, 130 nm Zn, 155 nm Cu and 180 nm Sn sputtered on an Ashai PV 200 glass substrate [1]. The film is slightly thicker than 1 μm with elemental ratios $[\text{Zn}]/[\text{Sn}] \cong 1.25$ and $[\text{Cu}]/([\text{Zn}]+[\text{Sn}]) \cong 0.85$. The energy conversion efficiency of a device with a nominally similar absorber was measured $\sim 5\%$. S2 and S3 were fabricated with co-evaporation method on soda lime glass substrates. The film thickness was 1.49 μm with $[\text{Zn}]/[\text{Sn}] \cong 1.32$ and $[\text{Cu}]/([\text{Zn}]+[\text{Sn}]) \cong 0.82$ for S2, and 1.3 μm with $[\text{Zn}]/[\text{Sn}] \cong 1.28$ and $[\text{Cu}]/([\text{Zn}]+[\text{Sn}]) \cong 0.87$ for S3. S3 was finished with CdS layer, ZnO bi-layer, Ni/Al grids and an MgF₂ antireflective coating. Details for the film growth and device processing can be found in Refs. [2] and [3]. A device with nominally same absorber of S2 has an energy conversion efficiency of $\sim 8\%$ and the efficiency of S3 was also $\sim 8\%$.

RESULTS AND DISCUSSIONS

Raman studies from front surface at room temperature

The effect of HP illumination was first examined at individual locations from the front surface. For each sample, after taking the Raman spectrum at LP 0.146 mW ($3.5 \times 10^4 \text{ W/cm}^2 \approx 3500 \text{ sun}$) shown in red solid curve in Fig. 1, the same spot was illuminated with 2.47 mW ($5.9 \times 10^5 \text{ W/cm}^2$) for 100 seconds, then the Raman spectrum was re-measured at LP under the same conditions, shown in green dash line. The high laser power was further increased to 4.5 mW ($1.1 \times 10^6 \text{ W/cm}^2$) for 36 second. Raman data collected again with LP were shown in blue dot line in Fig. 1. The illuminated spots showed some color change but no apparent ablation after 2.47 mW illumination. However, the 4.5 mW illumination resulted in local material ablation. In their initial states, all three samples exhibited similar Raman features: two main CZTSe Raman peaks at $195 - 196 \text{ cm}^{-1}$ and $172 - 173 \text{ cm}^{-1}$, and a weak CZTSe peak at $232 - 233 \text{ cm}^{-1}$ [4]; multiple weak peaks such as ~ 222 , ~ 245 and $\sim 251.5 \text{ cm}^{-1}$ forming a “mesa-like” band to the right of the $195 - 196 \text{ cm}^{-1}$ peak. The $\sim 222 \text{ cm}^{-1}$ peak is assigned to be a transverse optical (TO) Raman mode in E symmetry from kesterite structure based on theoretical calculations [5-7]. The $\sim 245 \text{ cm}^{-1}$ peak was reported to be CZTSe related both theoretically and experimentally [8-10]. There are three possible origins of the $\sim 251.5 \text{ cm}^{-1}$ peak: ZnSe at 253 cm^{-1} [11-13], Cu₂SnSe₃ at 251 cm^{-1} [4], and amorphous selenium (a-Se) at $\sim 250 \text{ cm}^{-1}$ [14]. Since the CZTSe films are fabricated in Se-rich condition, it is highly possible that surplus selenium is present in the films. CdS is known as the origin of the Raman line at 303.6 cm^{-1} from the finished device S3 [15].

After 2.47 mW illumination, as shown by the green dash curves in Fig. 1 (a) – (c), the two main CZTSe peaks 196 and 172 cm^{-1} experienced not only intensity reduction but also redshift for all three samples: 2.3 cm^{-1} for S1, 1.3 cm^{-1} for S2 and 0.5 cm^{-1} for S3. These changes suggest that HP illumination leads irreversible atomic bonds thermal expansion at the illuminated site. The weak features in the mesa-like band appear to smear out and weaken in both S1 and S2, but

in S2 a new feature at $\sim 262\text{ cm}^{-1}$ emerges, as shown in Figs. 1(b); whereas in S3, those weak features remained but their relative intensities changed, for example, the peaks at ~ 235 and 250.5 cm^{-1} became more apparent, as shown in Fig. 1(c).

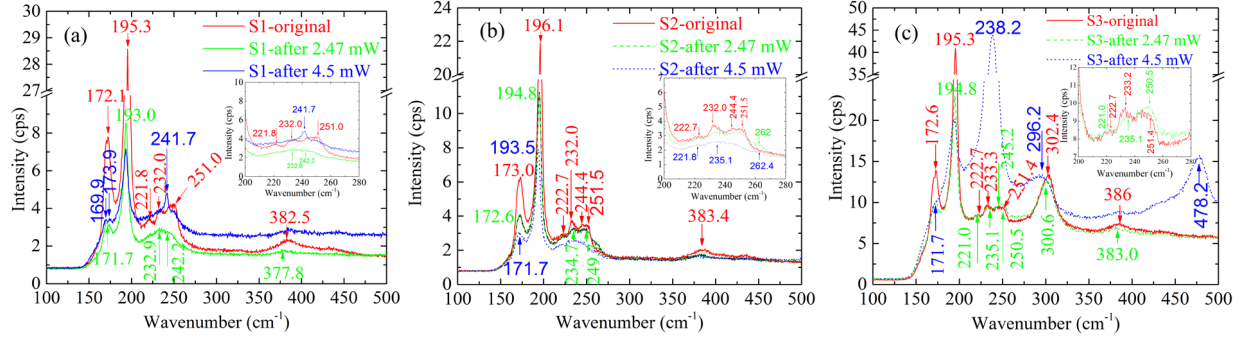


Figure 1. Raman spectra of CZTSe samples at 0.146 mW before and after being illuminated by high powers: (a) S1; (b) S2; (c) S3.

After 4.5 mW illumination, the main CZTSe peak experienced further intensity reduction, shown as the blue dot curves in Figs. 1 (a) – (c). For S1, the intensity of the 193 cm^{-1} peak is less than 20% of its original value before any HP illumination, and the 172 cm^{-1} mode becomes a weak shoulder from 168 to 178 cm^{-1} . However, for S2, the main CZTSe peak intensity only decreases by a factor of four, and the $\sim 172\text{ cm}^{-1}$ peak remains sharp. For the mesa-band, a MoSe₂ Raman mode emerges at 241.7 cm^{-1} in S1[16], but not in S2 and S3; no significant further change in S2 except for the slightly better resolved feather $\sim 262\text{ cm}^{-1}$, which turns out to be Cu_xSe_y mode coming from the periphery of the illuminated spot [17, 18]; in S3, a very strong sharp peak at 238.2 cm^{-1} appeared, accompanied by a second order peak at 478.2 cm^{-1} and a third order peak at $\sim 714\text{ cm}^{-1}$ (not shown), and a broad band at $\sim 296\text{ cm}^{-1}$. The $\sim 238\text{ cm}^{-1}$ peak in S3 is most likely the A1 mode of t-Se [14, 19]. It was shown that as a result of photo-crystallization, a broad band at $\sim 250\text{ cm}^{-1}$ and a shoulder at $\sim 235\text{ cm}^{-1}$ observed in an a-Se film became two resolved E symmetry mode at 233 cm^{-1} and A1 symmetry mode at 237 cm^{-1} of t-Se [14]. Our observations in S3 before and after the second HP illumination matches this transformation, which suggests the possibility that a-Se existed in the as-deposited CZTSe film. Obviously, the second HP illumination brought more qualitatively different changes to these samples. Changes in Raman spectra from all three CZTSe samples after the HP illumination indicated partial decomposition and plastic deformation of the materials. However, different samples responded rather differently to the HP illumination, indicating that seemingly similar CZTSe materials could differ significantly in their microscopic structures. The contrast between S1 and S2 suggests that the CZTSe structure prepared by co-evaporation seems to be more robust than that prepared by sputtering against HP illumination induced structural modifications.

2D Raman mapping was performed to examine the spatial extension of the local heating effect caused by the HP illumination on the CZTSe samples, as shown in Fig. 2 for the 2.47 mW illumination. One random spot from each sample surface was first illuminated by 2.47 mW for 100 seconds, Raman mapping was then acquired with 0.146 mW laser power from a square centered at the illuminated spot. For each sample, Raman intensity mapping reveals a dark circle for the 196 cm^{-1} peak, as shown in Figs. 2(a) – (c), confirming the intensity reduction of the CZTSe main Raman mode at 196 cm^{-1} . In the Raman mapping for S1, a Raman peak at $\sim 261\text{ cm}^{-1}$ was observed in a ring outside of the illumination site, as evident in Fig. 2(d), whereas in the mapping results of S2 and S3, the $\sim 261\text{ cm}^{-1}$ peak was not observed, as shown in Fig. 2(e) and (f).

The Raman mapping of the primary CZTSe mode at the 196 cm^{-1} reveals most directly the spatial extension the material being affected by the local heating. For S1, as shown in Fig. 2(a), beyond the darkest $\sim 1\text{ }\mu\text{m}$ circle (comparable to the laser spot size of $\sim 0.76\text{ }\mu\text{m}$) at the illumination site, a dark area with a diameter of $\sim 3\text{ }\mu\text{m}$, comparable to the size of the 261 cm^{-1} ring, also shows significantly lower intensity of the 196 cm^{-1} peak. On the other hand, 2.47 mW laser illumination only affects an area of about $1.5\text{ }\mu\text{m}$ diameter in S2 and even less than $1\text{ }\mu\text{m}$ diameter in S3. The difference between S1 and S2 seems to suggest that CZTSe absorber layer prepared by the sputtering method is more sensitive to the HP illumination than the film fabricated by the co-evaporation method. These two nominally similar films might have rather different thermal conductivities, which might be partially responsible to the different responses in structural change mentioned above.

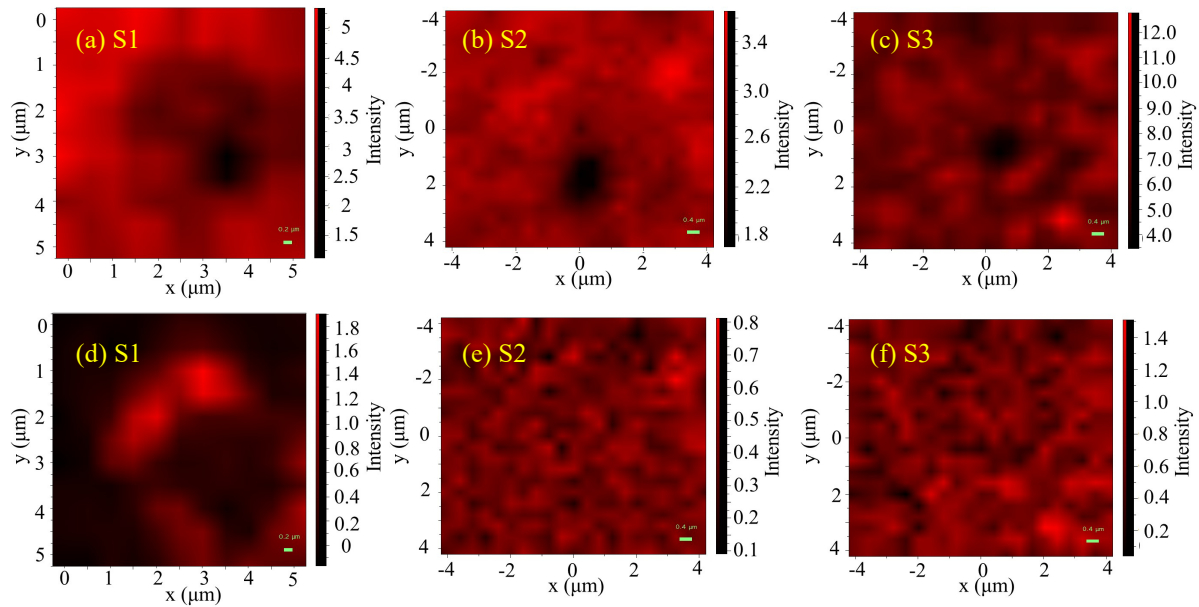


Figure 2. Raman mapping after one spot being illuminated by 2.47 mW for 100 s : (a) – (c) Raman mapping of 196 cm^{-1} peak; (d) – (f) Raman mapping of 261 cm^{-1} peak.

High temperature Raman studies from front surface

High temperature Raman spectra of a random spot from each sample were collected with a step of $20\text{ }^{\circ}\text{C}$ starting from room temperature using 0.147 mW laser power with a $50\times$ long working distance lens. Raman spectra at representative temperatures were shown in Fig. 3. For all three samples, the main CZTSe peak at $\sim 196\text{ cm}^{-1}$ experiences redshift, intensity reduction and linewidth broadening with increasing temperature. The mesa-like band from 220 cm^{-1} to 250 cm^{-1} becomes narrower, and finally forms a sharp and strong peak centered at $\sim 237\text{ cm}^{-1}$, together with its second order mode $\sim 478\text{ cm}^{-1}$, when temperature is higher than $600\text{ }^{\circ}\text{C}$. The local temperature of the illuminated site induced by HP illumination can be estimated by comparing the Raman shift of the main CZTSe Raman peak between the lower and high power spectrum. Based on the red-shifts observed with the 2.47 mW illumination: 4.9 (S1), 3.6 (S2), and 2.2 (S3) cm^{-1} , and the temperature dependences shown in Fig. 3, the local temperature reaches about $\sim 280\text{ }^{\circ}\text{C}$ in S1, $\sim 260\text{ }^{\circ}\text{C}$ in S2, and $\sim 200\text{ }^{\circ}\text{C}$ in S3. The results of the higher power 4.5 mW illumination are inappropriate for such estimate, because the CZTSe material at the illumination site was either ablated or converted into t-Se.

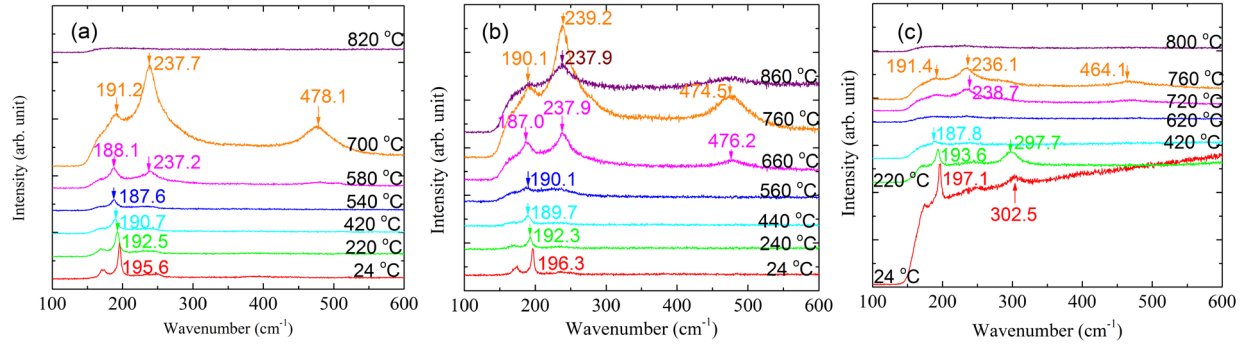


Figure 3. Raman spectra measured at different temperatures: (a) S1; (b) S2; (c) S3.

Raman studies from cleaved edge at room temperature

Raman spectra were also measured from cleaved edge with laser beam focused to different depths of the sample: Mo layer, Mo-CZTSe boundary, body of film, and film-air boundary. Because of the limitation of the laser spot size, these measurements can only reveal the changes qualitatively. In Fig. 4, one can clearly see the spectral feature variation with the depth of the film. For example, MoSe₂ is the dominant component at the substrate-film boundary with Raman modes at 169, 242, 286 and 351 cm⁻¹ in S1. When moving toward the front surface, the MoSe₂ related peaks gradually diminish, whereas the CZTSe peaks at 196 cm⁻¹ and 172 cm⁻¹ grow. In contrast, no Raman signal from MoSe₂ was observed near the substrate in S2. The measured cleaved edge spots were illuminated at 2.47 mW for 100 seconds and further 4.5 mW for 36 seconds. Fig. 5 shows the Raman spectra collected from these spots with 0.147 mW after HP illumination. In addition to redshift, Cu_xSe_y Raman mode appeared from substrate of S1 and throughout the film depth of S2. For S1, many other new peaks were detected at its substrate and CZTSe film boundary, such as SnSn peak 185.6 cm⁻¹, ZnSe peak at 202.6 cm⁻¹, and molybdenum oxide Raman modes at 729.3 cm⁻¹ and 819.0 cm⁻¹. With the coexistence of Cu_xSe_y, ZnSe, SnSe and MoSe₂ near the substrate and film boundary, this result confirms the process $2\text{Cu}_2\text{ZnSnSe}_4 + \text{Mo} \rightarrow 2\text{Cu}_2\text{Se} + 2\text{ZnSe} + 2\text{SnSe} + \text{MoSe}_2$ predicted in Ref. [20]. However, in Fig. 5(b), only secondary phases Cu₂SnSe₃ /a-Se and Cu_xSe_y but no ZnSe or MoSe₂ was found from S2. These observations again indicate the microscopic structure of the polycrystalline CZTSe film could vary substantially with deposition method.

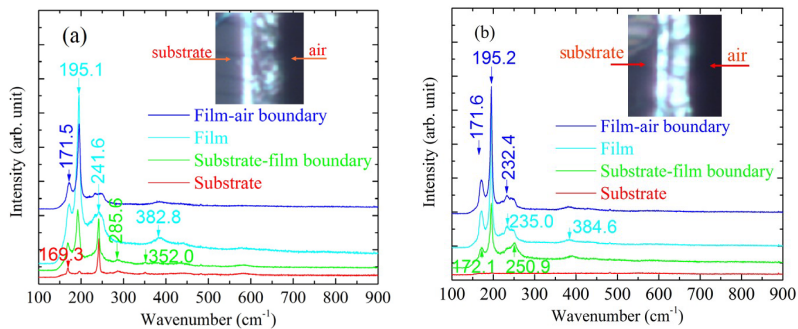


Figure 4. Raman spectra of CZTSe samples measured from cleaved edge: (a) S1; (b) S2.

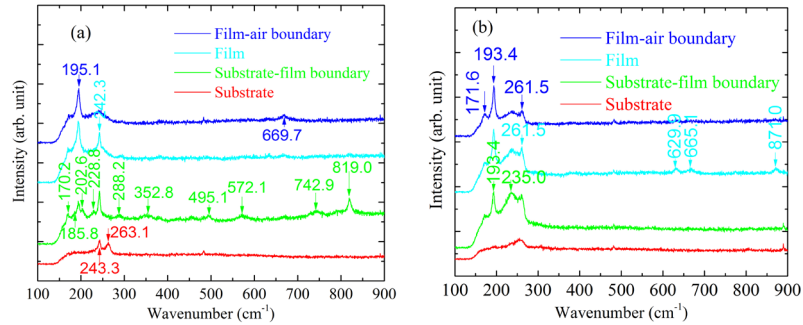


Figure 5. Raman spectra of CZTSe samples measured from cleaved edge after being illuminated by 4.5 mW: (a) S1; (b) S2.

SUMMARY

Combining spatially-resolved HP and HT μ -Raman spectroscopy, CZTSe films, which appear very similar with conventional characterization tools, were found significantly different in microscopic structures. HP illumination brought different changes to films prepared by different methods. Different thermal conductivities of the samples were demonstrated by HP Raman mapping, suggesting different microscopic structures. HT Raman measurements reveals the different decomposition processes of the three samples. In general, the combination of high power and high temperature Raman study can offer an effective approach to examine the microscopic structural variations of the complex alloys like CZTSe, even when they are macroscopically similar.

ACKNOWLEDGMENTS

We are very grateful to Dr. I. Repins (NREL) for providing the co-evaporated samples and helpful discussions. Y.Z. acknowledges the support of Bissell Distinguished Professorship.

REFERENCES

- [1] L. Grenet, R. Fillon, G. Altamura, H. Fournier, F. Emieux, P. Faucherand, *et al.*, *Sol. Energy Mater. Sol. Cells*, **126**, 135 (2014).
- [2] I. Repins, C. Beall, N. Vora, C. DeHart, D. Kuciauskas, P. Dippo, *et al.*, *Sol. Energy Mater. Sol. Cells*, **101**, 154 (2012).
- [3] N. Vora, J. Blackburn, I. Repins, C. Beall, B. To, J. Pankow, *et al.*, *J. Vac. Sci. Technol. A*, **30**, 051201 (2012).
- [4] M. Altosaar, J. Raudoja, K. Timmo, M. Danilson, M. Grossberg, J. Krustok, *et al.*, *Phys. Status Solidi A*, **205**, 167 (2008).
- [5] A. Khare, B. Himmetoglu, M. Johnson, D. J. Norris, M. Cococcioni, and E. S. Aydil, *J. Appl. Phys*, **111**, 083707 (2012).
- [6] M. Dimitrievska, A. Fairbrother, E. Saucedo, A. Pérez-Rodríguez, and V. Izquierdo-Roca, *Appl. Phys Lett*, **106**, 073903 (2015).
- [7] T. Gürel, C. Sevik, and T. Çağın, *Phys. Rev. B*, **84**, 205201 (2011).
- [8] M. Grossberg, J. Krustok, J. Raudoja, K. Timmo, M. Altosaar, and T. Raadik, *Thin Solid Films*, **519**, 7403 (2011).

- [9] M. Grossberg, J. Krustok, K. Timmo, and M. Altosaar, *Thin Solid Films*, **517**, 2489 (2009).
- [10] A. Redinger, K. Hönes, X. Fontané, V. Izquierdo-Roca, E. Saucedo, N. Valle, *et al.*, *Appl. Phys. Lett.*, **98**, 101907 (2011).
- [11] H. Li, B. Wang, and L. Li, *J. Alloys and Compounds*, 506, 327 (2010).
- [12] J. Scott, T. Damen, W. Silfvast, R. Leite, and L. Cheesman, *Opt. Commun.*, **1**, 397 (1970).
- [13] C. Shan, Z. Liu, X. Zhang, C. Wong, and S. Hark, *Nanotechnology*, **17**, 5561 (2006).
- [14] V. V. Poborchii, A. V. Kolobov, and K. Tanaka, *Appl. Phys. Lett.*, **72**, 1167 (1998).
- [15] Q. Chen and Y. Zhang, *Appl. Phys. Lett.*, **103**, 242104 (2013).
- [16] T. Sekine, M. Izumi, T. Nakashizu, K. Uchinokura, and E. Matsuura, *J. Phys. Soc. Jpn.*, **49**, 1069 (1980).
- [17] M. Ishii, K. Shibata, and H. Nozaki, *J. Solid State Chem.*, **105**, 504 (1993).
- [18] F. Luckert, D. Hamilton, M. Yakushev, N. Beattie, G. Zoppi, M. Moynihan, *et al.*, *Appl. Phys. Lett.*, **99**, 062104 (2011).
- [19] V. V. Poborchii, A. V. Kolobov, J. Caro, V. V. Zhuravlev, and K. Tanaka, *Chem. Phys. Lett.*, **280**, 17 (1997).
- [20] J. J. Scragg, P. J. Dale, D. Colombara, and L. M. Peter, *ChemPhysChem*, **13**, 3035, (2012).